Inorg. Chem. **2005**, *44*, 5890–5896

Stabilization of the Thermodynamically Favored Polymorph of Cadmium Chalcogenide Nanoparticles CdX (X = S, Se, Te) in the Polar Mesopores of SBA-15 Silica

Maekele Yosef,[†] Andreas K. Schaper,[‡] Michael Fröba,[§] and Sabine Schlecht*,[†]

Fachbereich Chemie, Philipps-Universität Marburg, 35032 Marburg, Germany, Wissenschaftliches Zentrum für Materialwissenschaften, Philipps-Universität Marburg, 35032 Marburg, Germany, and Institut für Anorganische und Analytische Chemie, Justus-Liebig-Universität Giessen, 35392 Giessen, Germany

Received April 6, 2005

A versatile synthetic approach to cadmium chalcogenide nanoparticles in the mesopores of SBA-15 silica as a host matrix was developed. The use of cadmium organochalcogenolates of the type $Cd(XPh)_2 \cdot TMEDA$ (X = S, Se, Te) allowed the preparation of nanoparticles of all three cadmium chalcogenides following the same experimental protocol. Particles of CdS, CdSe, and CdTe with a particle size of 7 nm were prepared from this class of single-source precursors. The incorporation of the precursor molecules into the pores was achieved by melt infiltration at a temperature of 140 °C. Subsequent pyrolysis of the precursors in the mesopores yielded the semiconductor particles. Owing to the high polarity of the silanol-covered pore walls, which lower the surface energy of the particles to a large extent, the dimorphic cadmium chalcogenides are obtained in their thermodynamically favored modifications; e.g., CdS particles crystallize in the wurtzite type, CdTe particles are obtained in the zinc blende structure, and CdSe (where no unambiguous preference exists) crystallizes as a "mixture" of both structures with a rather random stacking sequence.

Introduction

One of the major challenges in nanoparticle synthesis is the precise control over the size and shape of the produced nanoscale materials. Thus, a large number of syntheses in aqueous and nonaqueous media involving surface-capping additives have been developed, which can provide monodisperse nanoparticles of metals,[1,2] ceramics,[3] or semiconductors.[4] A different kind of concept for size control by steric barriers that physically limit the growth of the product particles is the use of ordered porous templates[5] where the pore array can act as a spatially confined reaction vessel. In addition, the polar protic walls of mesoporous silica[6] provide the interesting opportunity to control not only the particle size but also the volume structure of the particle. Similar to the structure-determining effect of a protic polar reagent such as water on the volume structure of II/VI semiconductor nanoparticles,[7,8] the silanol groups of the walls of mesoporous silica can also be expected to induce the formation of the thermodynamically favored bulk phase of the respective semiconductor by an efficient reduction of the surface energy and of the disorder phenomena related to the surface of the nanoparticles (Scheme 1).

Thus, the aim of our investigations was the elucidation of the phase stabilities of the nanoscale cadmium chalcogenides CdS, CdSe, and CdTe in this polar environment of the pores of mesoporous silica SBA-15. It can be expected that cadmium chalcogenide particles in the mesopores of SBA-

* To whom correspondence should be addressed. E-mail: schlecht@chemie.uni-marburg.de. Fax: +49-(0)6421−2825653.
† Fachbereich Chemie, Philipps-Universität Marburg.
‡ Wissenschaftliches Zentrum für Materialwissenschaften, Philipps-Universität Marburg.
§ Justus-Liebig-Universität Giessen.

(1) Puntes, V. F.; Krishnan, K.; Alivisatos, A. P. *Top. Catal.* **2002**, *19*, 145.
(2) Schmid, G. In *Nanoscale Materials in Chemistry*; Klabunde, K., Ed.; Wiley: New York, 2001; pp 15−59.
(3) Niederberger, M.; Pinna, N.; Polleux, J.; Antonietti, M. *Angew Chem., Int. Ed.* **2004**, *43*, 2270.
(4) Green, M.; O'Brien, P. *Chem. Commun*. **1999**, 2235.
(5) Kresge, C. T.; Leonowicz, M. E.; Roth, W. J.; Vartulli, J. C.; Beck, J. S. *Nature* **1992**, *359*, 710.
(6) Moller, K.; Bein, T. *Chem. Mater*. **1998**, *10*, 2950.
(7) Zhang, H.; Gilbert, B.; Huang, F.; Banfield, J. F. *Nature* **2003**, *424*, 1025.
(8) Zhang, H.; Huang, F.; Gilbert, B.; Banfield, J. F. *J. Phys. Chem. B* **2003**, *107*, 13051.

10.1021/ic050517h CCC: $30.25 © 2005 American Chemical Society
Published on Web 07/08/2005

Scheme 1. (a) Phase Transition into the Thermodynamically Favored Polymorph, Induced by Water as a Polar Medium; (b) Formation of Nanoparticles of the Thermodynamically Stable Phase by Precursor Thermolysis in the Polar Pores of SBA-15 Silica

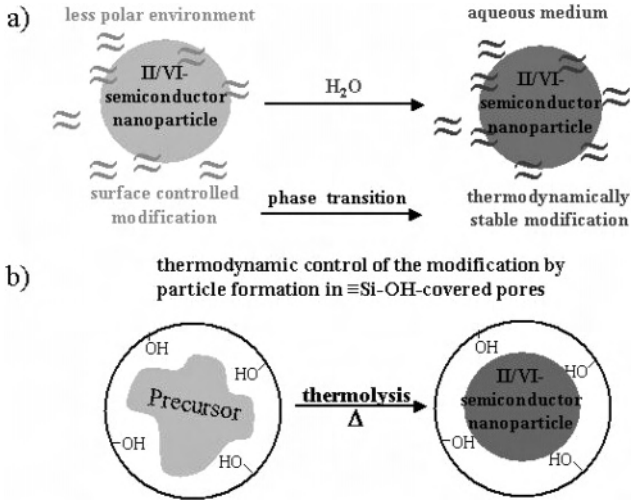

15 silica follow the phase stabilities of the bulk chalcogenides CdS, CdSe, and CdTe, where the wurtzite polymorph is found for CdS and CdSe whereas the cubic zinc blende structure is thermodynamically favored for CdTe.[9]

To make the synthetic approach versatile and equally valuable for all three cadmium chalcogenides, the incorporation of the reactands into the pores should not require any specific chemical binding interaction of the pore wall with the precursor system. If a generally applicable physical incorporation is chosen, a complete class of compounds can be produced in nanocrystalline form following the same experimental protocol. This last aspect is highly advantageous for a comparative study of thermodymanic control on the volume structure of the product particles.

In the present work, the feasability of this concept for the preparation of nanoscale cadmium chalcogenides CdX (X = S, Se, Te) from an easily accessible family of molecular precursors was investigated. According to the principle of a general physical incorporation of the precursor into the pores, a class of precursor molecules with rather uniform physical properties (e.g., solubility, melting point) and decomposition characteristics was chosen and base adducts of cadmium organochalcogenolates of the type $Cd(XPh)_2$·TMEDA (X = S, Se, Te; TMEDA = tetramethylethylenediamine) proved to be suitable candidates for this synthetic strategy.

Results and Discussion

Since the introduction of mesoporous materials in 1992,[5] these materials have provided a number of new synthetic pathways to nanostructured composites with a second compound of choice in the ordered pore system of the silica.[6] Different mesoporous silicas with a hexagonal pore structure such as MCM-41 or SBA-15 have mostly been used as hosts to accommodate semiconductor nanostructures such as Ge,[10] SiGe,[11] (Cd,Mn)S,[12] (Cd,Mn)Se[13] (Zn,Mn)S,[14] CdSe,[15] or Cu_2Te.[16] The pore walls of mesoporous SBA-15 or MCM-41 are covered by terminal silanol groups ≡SiOH, which make them a highly polar and fairly acidic host compound for any guest to be incorporated. On the other hand, the polar character of a pore wall containing a large number of ≡SiOH functionalities is highly advantageous for the minimization of the surface energy of an incorporated nanoparticle of, e.g., a cadmium chalcogenide.

The choice of the precursor system was governed by two principal considerations:

(i) Can the same type of compound with the same molecular structure and the same decomposition pathway be used for all chalcogenides CdS, CdSe, and CdTe?

(ii) Can the precursor easily be incorporated into the pores by simple melting?

One class of compounds that is accessible for all chalcogens and that is known to allow melting without decomposition are organochalcogenolates of transition metals.[17] In the case of the zinc chalcogenides ZnSe and ZnTe, the respective chalcogenolate precursors $Zn(XPh)_2$·TMEDA (X = Se, Te) were successfully applied for solution-phase syntheses of capped nanoscale particles in trioctylphosphine oxide.[18] Surprisingly, the analogous cadmium compounds have not been described so far, although similar properties in decomposition reactions leading to cadmium chalcogenide nanoparticles can be expected. Starting from this consideration, a straightforward synthesis for pure compounds of the series $Cd(XPh)_2$·TMEDA (X = S, Se, Te) was worked out. First, it became apparent that the preparation of the zinc compounds starting from LiXPh (X = Se, Te) and $ZnCl_2$ could not be transferred to cadmium chemistry in an analogous manner because the cadmium halides and the cadmium organochalcogenolates differ too strongly from their zinc counterparts with respect to their solubilities and no pure products could be obtained. Hence, a synthesis that avoids the precipitation of an alkali-metal halide from the cadmium salt proved to be the better approach. As already described for an alternative synthesis of $Zn(SePh)_2$·TMEDA,[19] group 12 halides react very cleanly with silylated chalcogenolates under the elimination of trimethylsilyl chloride as a volatile byproduct (eq 1). The silylated derivatives of phenylthiolate,[20] -selenolate,[21] and -tellurolate[22] were used to prepare

(9) Holleman, A.; Wiberg, E. *Lehrbuch der Anorganischen Chemie*, 101st ed.; de Gruyter: Berlin, 1995.

(10) Leon, R.; Margolese, D.; Stucky, G.; Petroff, P. M. *Phys. Rev. B* **1995**, *52*, R2285. Schlecht, S.; Yosef, M.; Fröba, M. *Z. Anorg. Allg. Chem.* **2004**, *630*, 864.

(11) Tang, Y. S.; Cai, S.; Jin, G.; Duan, J.; Wang, K. L.; Soyez, H. M.; Dunn, B. S. *Appl. Phys. Lett.* **1997**, *71*, 2449.

(12) Chen, L.; Klar, P. J.; Heimbrodt, W.; Brieler, F.; Fröba, M. *Appl. Phys. Lett.* **2000**, *76*, 3531. Brieler, F.; Fröba, M.; Chen, L.; Klar, P. J.; Heimbrodt, W. *Chem. Eur. J.* **2002**, *8*, 185.

(13) Chen, L.; Falk, H.; Klar, P. J.; Heimbrodt, W.; Brieler, F.; Fröba, M.; Krug von Nidda, H.-A.; Loidl, A.; Chen, Z.; Oka, Y. *Phys. Status Solidi B* **2002**, *229*, 31.

(14) Brieler, F.; Grundmann, P.; Fröba, M.; Chen, L.; Klar, P. J.; Heimbrodt, W.; Krug von Nidda, H.-A.; Kurz, T.; Loidl, A. *J. Am. Chem. Soc.* **2004**, *126*, 797.

(15) Parala, H.; Winkler, H.; Kolbe, M.; Wohlfahrt, A.; Fischer, R. A.; Schmechel, R.; von Seggern, H. *Adv. Mater.* **2000**, *12*, 1050.

(16) Kowalchuk, C. M.; Schmid, G.; Meyer-Zaika, W.; Huang, Y.; Corrigan, J. F. *Inorg. Chem.* **2004**, *43*, 173.

(17) Arnold, J. *Prog. Inorg. Chem.* **1995**, *43*, 353.

(18) Jun, Y.; Koo, J.-E.; Cheon, J. *Chem. Commun.* **2000**, 1243. Jun, Y.; Choi, C.-S.; Cheon, J. *Chem. Commun.* **2001**, 101.

(19) Pfistner, H.; Fenske, D. *Z. Anorg. Allg. Chem.* **2001**, *627*, 575.

Table 1. Melting Points and Decomposition Characteristics of $Cd(SPh)_2$·TMEDA, $Cd(SePh)_2$·TMEDA, and $Cd(TePh)_2$·TMEDA

	$Cd(SPh)_2$· TMEDA	$Cd(SePh)_2$· TMEDA	$Cd(TePh)_2$· TMEDA
melting point (°C)	106	127	101
first decomp. step (°C)	314	305	196
second decomp. step (°C)	387	351	263

the whole series of cadmium phenylchalcogenolates (eqs 2−4). To make $CdCl_2$ more soluble in toluene, 2.5 equiv of TMEDA was added beforehand, leading to the formation of the base adduct $CdCl_2$·2TMEDA as a more reactive intermediate for the reaction with the silylated organochalcogenolates. The solution of $CdCl_2$·2TMEDA was held at room

$$ZnCl_2 + 2Me_3SiSePh \xrightarrow{+TMEDA} Zn(SePh)_2{*}TMEDA + 2Me_3SiCl \quad (1)$$

$$CdCl_2 + 2Me_3SiSPh \xrightarrow{+TMEDA} Cd(SPh)_2{*}TMEDA + 2Me_3SiCl \quad (2)$$

$$CdCl_2 + 2Me_3SiSePh \xrightarrow{+TMEDA} Cd(SePh)_2{*}TMEDA + 2Me_3SiCl \quad (3)$$

$$CdCl_2 + 2Me_3SiTePh \xrightarrow{+TMEDA} Cd(TePh)_2{*}TMEDA + 2Me_3SiCl \quad (4)$$

temperature while 2 equiv of Me_3SiSPh, $Me_3SiSePh$, or $Me_3SiTePh$ was added. The reaction mixtures were stirred overnight, the solvent was removed under vacuum, and the resulting solids were recrystallized from a toluene solution at −24 °C. Very pure organochalcogenolates $Cd(XPh)_2$·TMEDA were produced in good yield by this method, and suitable crystals for X-ray crystal structure analysis were obtained for $Cd(SPh)_2$·TMEDA and for $Cd(SePh)_2$·TMEDA. Crystal structure determinations revealed that both compounds are isotypic and crystallize in the monoclinic system in the space group $P2_1/c$ with four molecules in the unit cell. Monomeric complexes with a rather unusual arrangement of two nitrogen atoms and two chalcogen atoms attached to the cadmium center are found in the crystal structures. Details on the crystal structures and on the crystal structure determination are given in the Supporting Information.

To find the most suitable thermal treatment of the cadmium organochalcogenolate precursors for their decomposition into cadmium chalcogenides, calorimetric investigations of the decomposition procedure were performed prior to the thermolyses in the silica host. The investigations showed that all three precursor compounds degraded through two distinct endothermal events. The individual decomposition characteristics for the different organochalcogenolates of cadmium are given in Table 1. In all cases, we recorded X-ray powder diffraction patterns after the first step of the decomposition,

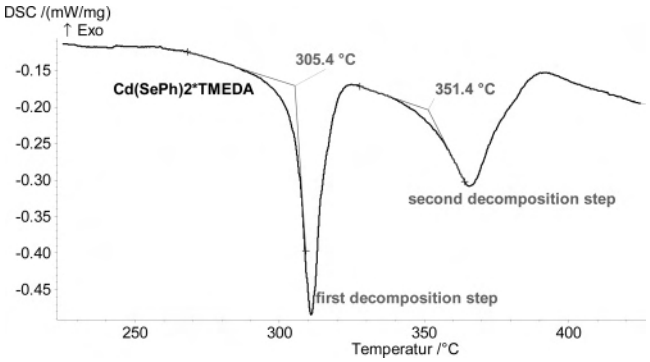

Figure 1. DSC diagram of the thermolysis of $Cd(SePh)_2$·TMEDA, indicating two principal decomposition steps of the precursor.

which is related to the loss of TMEDA ligand, and found X-ray amorphous products that still contained a significant amount of organic material, which could be verified by elemental analysis. No reflections of already formed grains of cadmium chalcogenides were detected at this stage of thermolysis. However, a fully developed set of reflections of the respective cadmium chalcogenide were present in all cases after the second decomposition step, which comprises the elimination of arylchalcogenide Ph_2E, was completely finished. These experiments made clear that the formation of grains of the semiconductor is limited to this second event. Immediately following the second endothermic signal, a weaker exothermic peak at $T_{cryst} = 382$ °C, which belongs to this decomposition step, is observed and can be attributed to the crystallization of the primary grains of the semiconductor into nanoscale-ordered particles. The differential scanning calorimetry (DSC) analysis of $Cd(SePh)_2$·TMEDA in the temperature range where the decomposition occurs is shown as one representative example in Figure 1. The melting points of the chalcogenolate precursors proved to be a second important aspect (Table 1). All three compounds show melting points below 150 °C and can thus easily be incorporated into the pores of SBA-15 in the liquid state without decomposition.

The infiltration of the molten precursors into SBA-15 silica was conducted in the following way: calcined SBA-15 and an equal amount of the chalcogenolate precursor were slowly heated to ∼140 °C. Gradually, the precursor melt was incorporated into the pores of SBA-15 silica. The samples were held at a final temperature of pyrolysis of 350 °C for 14−16 h. This prolonged heating also leads to complete decomposition of the thiolate complex that has a nominally higher decomposition temperature (Table 1). During the pyrolysis of the precursors, the condensation of the volatile byproduct Ph_2S, Ph_2Se, or Ph_2Te at the cold top part of the Schlenk tube was observed, and the obtained diphenylchalcogenides could be identified by NMR spectroscopy. After pyrolysis had been completed, the samples were washed with hexane and tetrahydrofuran to remove all organic residues potentially present on the surface of the composites. The remaining powders were characterized by energy-dispersive X-ray (EDX) analysis, powder diffractometry, and transmission electron microscopy (TEM). For all three nanocomposites CdS@SBA-15, CdSe@SBA-15, and CdTe@SBA-15,

(20) Kuwajima, I.; Abe, T. *Bull. Chem. Soc. Jpn.* **1978**, *51*, 2183.
(21) Clarembeau, M.; Cravador, A.; Dumont, W.; Haresi, L.; Krief, A.; Lucchetti, J.; van Ende, D. *Tetrahedron* **1985**, *41*, 4793.
(22) Sasaki, K.; Aso, Y.; Otsubo, T.; Ogura, F. *Tetrahedron Lett.* **1985**, *26*, 453.

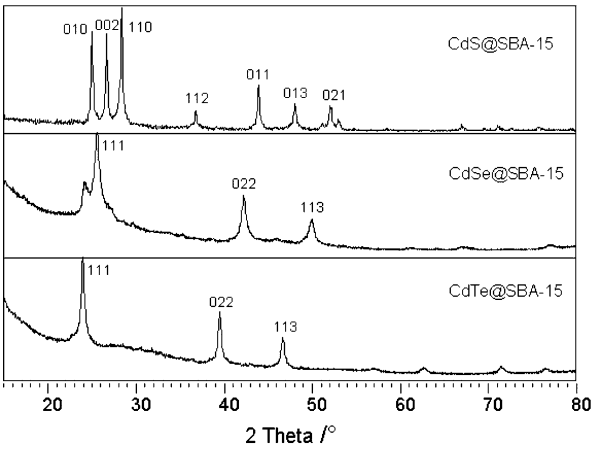

Figure 2. X-ray powder diffraction patterns of the nanocomposites CdS@SBA-15, CdSe@SBA-15, and CdTe@SBA-15.

EDX investigations confirmed a 1:1 ratio of cadmium and the respective chalcogen in the products. The close similarity of the preparations of the different nanocomposites directly in the template pores provides an optimum comparability of the formation conditions of the different cadmium chalcogenides. Thus, the same influence of the polar pore walls and the same sequence of pyrolytic steps can be expected to lead to the same degree of thermodynamic control over the different cadmium chalcogenide products.

The obtained nanocomposite products CdS@SBA-15, CdSe@SBA-15, and CdTe@SBA-15 were characterized by X-ray powder diffraction. The diffraction patterns depicted in Figure 2 show the reflections of the cadmium chalcogenides in the amorphous matrix. All samples exhibit high crystallinity of the nanoparticles incorporated into the mesopores of the silica host. The different cadmium chalcogenides are formed in different modifications. Cadmium telluride was obtained in the zinc blende structure, cadmium sulfide in the wurtzite structure, and cadmium selenide as a mixture of the two polymorphs. Using Scherrer's equation,[23] a particle size of 8 ± 2 nm was found for CdS and CdTe, which is in accordance with the particle size determined by TEM investigations. No particle size for CdSe was calculated from the half-width of the reflection for the reasons given below. It was crucial to use recrystallized, very pure precursors in these experiments because the presence of impurities in the chalcogenolates always leads to the formation of the wurtzite phase only.

The cadmium chalcogenide nanocomposites were further investigated by TEM to gain insight into the degree of filling of the pores and to get additional information about the possible presence of nonnanoscale material outside the pores and on the surface of the template. As can be seen from Figure 3, showing bright-field images of an array of empty pores of SBA-15 and an array of filled pores of CdTe@SBA-15 as well as a cross section of the partially filled pores in this composite, no additional material outside the channels was found. Overview images of larger assemblies of CdTe@SBA-15 also showed no separate phase of macroscale

(23) Guinier, A. *X-ray Diffraction in Crystals, Imperfect Crystals and Amorphous Bodies*; Dover: New York, 1994; pp 121−130.

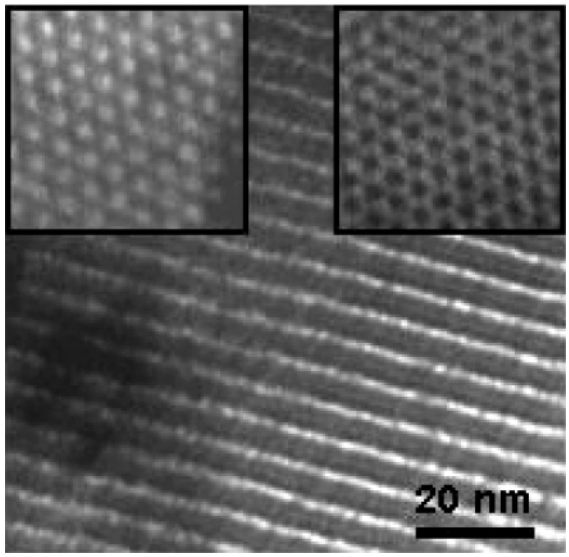

Figure 3. Cross section of partially filled pores in CdTe@SBA-15. Top view of an array of empty pores of SBA-15 (left inset) and of an array of pores filled with CdTe (right inset).

CdTe outside the template. Corresponding TEM micrographs of CdSe@SBA-15 and of CdS@SBA-15 are shown in Figure 4. In these cross-sectional views, partially filled pores with incorporated CdSe and CdS can be identified. To identify the material within the pores without ambiguity, we conducted nanobeam diffraction experiments on filled regions of CdSe@SBA-15 grains (Figure 5). The diffraction patterns were taken from two circular regions of 5 nm diameter as indicated in Figure 5. After appropriate tilting, nanobeam diffraction patterns for zone axis [100] of the cubic modification of CdSe and for zone axis [111] of the cubic phase (or [001] of the wurtzite phase) in the filled pores of SBA-15 silica could be obtained. These nanobeam diffraction experiments indicate that the filling of the pores of the mesoporous host is unambiguously CdSe.

To obtain free-standing particles of the cadmium chalcogenides and to investigate the influence of the template walls on the structure of the particles, the template was removed by dissolution in a strong base such as aqueous NaOH or KOH. As-obtained nanoparticles of CdS were yellow in color, whereas brownish CdSe and gray CdTe were obtained. The remaining pure particles of the respective cadmium chalcogenides were investigated by TEM to study their morphology and their structural identity. In Figure 6, high-resolution TEM (HRTEM) micrographs of as-obtained unprotected particles of CdTe and CdSe are shown. It can be seen from the HRTEM pictures and from electron diffraction experiments (see inset) that the free particles show very good crystallinity and that CdTe is still in the cubic sphalerite structure. In the case of CdSe, the strong reflections of the cubic phase are dominant, whereas the reflections of the wurtzite polymorph can only vaguely be identified by our electron diffraction experiments because they are intrinsically of lower intensity. Because of the loss of the protective surface of the template, the nanoparticles immediately form higher aggregates of individual particles to minimize their surface energy. Because the overall polarity and the capability

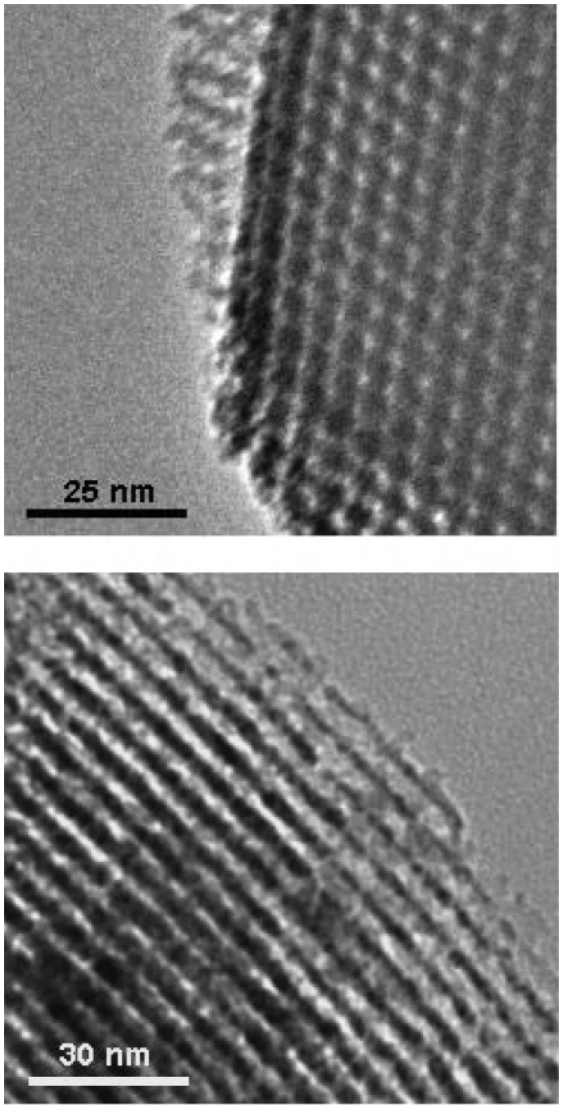

Figure 4. Top view of partially filled pores of CdSe@SBA-15 (top). Cross-sectional view of partially filled pores of CdS@SBA-15 (bottom).

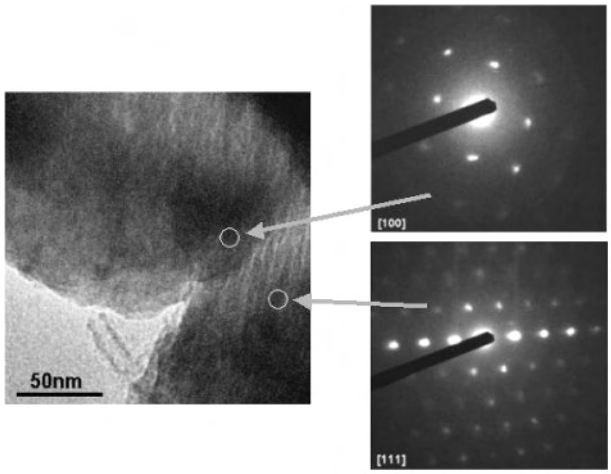

Figure 5. Overview of CdSe@SBA-15 grains with partially filled pores. White circles indicate the two regions where nanobeam diffraction patterns (beam diameter $d = 5$ nm) were taken along zone axis [100] (top) and zone axis [111] (bottom) of the zinc blende modification.

to compensate the extra surface energy of the nanoparticles are similar for silanol groups and for the aqueous bases used

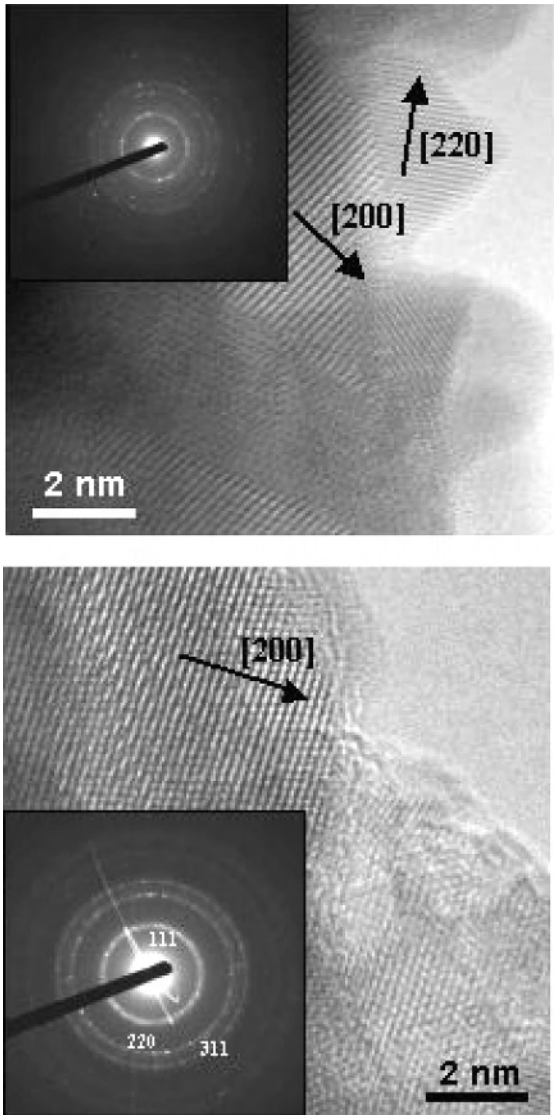

Figure 6. HRTEM micrograph and electron diffraction pattern of isolated particles of CdTe (top) and CdSe (bottom).

to dissolve the template, no structural changes were observed, not even for CdSe, where a phase transition to the thermodynamically favored pure wurtzite structure could be imagined. The effect of a polar capping, e.g., by water, on nanoparticles of the II/VI semiconductor family such as CdSe or ZnS is well established in the literature and was investigated theoretically as well as experimentally.[7,8,24,25] In all of these cases, the wurtzite structure is considered thermodynamically favored[26] and the occurrence of sphalerite particles was assigned to an additional stabilization of the isotropic modification by polar surface interactions and the rather spherical shape of very small grains.[7,8,25]

Phase transitions and phase stability in cadmium chalcogenide nanoparticles of 3−10 nm size have been the subject of continuing investigations for more than a decade.[27−29] In a number of cases, not only particles with the crystal structure

(24) Rabani, E. *J. Chem. Phys.* **2001**, *115*, 1493.
(25) Leung, K.; Whaley, K. B. *J. Chem. Phys.* **1999**, *110*, 11012.
(26) On a possible thermodynamic preference of the zinc blende structure: Yeh, C. Y.; Lu, Z. W.; Froyen, S.; Zunger, A. *Phys. Rev. B* **1992**, *46*, 10086.

of one of the two common polytypes (zinc blende or wurtzite) but also nanoparticles with domains of zinc blende and wurtzite within the same particle were observed.[27−29] It was shown that such intergrowth, caused by either stacking faults or twin borders in the nanoscale crystallite, leads to diffraction patterns with the same kind of overlapping reflections as those of a mixture of separate crystallites of the same size.[27] Thus, the "mixture" of zinc blende and wurtzite obtained for the CdSe particles can stem from (i) a real mixture of separate particles of the cubic and hexagonal polymorphs, (ii) from particles consisting of domains of a polytype with a stacking sequence different from strict ABCABC and strict ABABAB (e.g., ABABCBCABCB with a longer translational period),[27,30] or (iii) random stacking faults in a zinc blende type, leading to layers of wurtzite type plane stacking (e.g., ABCABCABAB). All three possibilities have already been observed in cadmium chalcogenide nanocrystals. Especially in the case of CdSe, there is apparently no preference for a certain polytype *in small nanoparticles*,[27] and the stacking along [111] of the cubic phase seems to be almost random. In light of these observations, it becomes much more obvious why there is no driving force for a room-temperature phase transition of the particles into pure wurtzite either in the silanol covered pores or in aqueous solution.

Experimental Section

All synthetic manipulations were carried out under exclusion of air and moisture in an argon atmosphere. All solvents were dried and freshly distilled under argon prior to use. $CdCl_2$, Me_3SiCl, Ph_2Te_2, Ph_2Se_2, Ph_2S_2, and Li[Et_3BH], 1 M in THF, were purchased from Aldrich and used as obtained. Powder diffraction patterns were recorded on a Philips X′Pert diffractometer using Cu Kα radiation. Recording times of 48 h were applied for the nanocomposites. $Me_3SiTePh$, $Me_3SiSePh$, and Me_3SiSPh and SBA-15 silica with a pore diameter of $d = 7$ nm were synthesized according to literature procedures.[14,20−22]

TEM was performed using a JEOL JEM 3010 electron microscope (300 kV; LaB_6 cathode). The samples were finely dispersed in ethanol. One drop of the dispersion was placed on a carbon-coated copper grid and allowed to dry, leaving the crystallites in a random orientation on the support film.

Thermal analyses were carried out under a dynamic argon atmosphere with a Netzsch Pegasus 404 DSC calorimeter.

Preparation of Cd(SPh)$_2$·TMEDA. In a Schlenk flask, 0.137 g (0.75 mmol) of $CdCl_2$ and 6 mL of TMEDA were dissolved in 30 mL of toluene. An amount of 0.273 g (1.5 mmol) of Me_3SiSPh in 20 mL of toluene was added at room temperature, and the resulting reaction mixture was stirred for 8 h. The mixture was filtered to remove a small quantity of a white solid, and the filtrate was evaporated to about half of its volume under reduced pressure. The resulting light yellow solution was stored at −24 °C to give colorless crystals of Cd(SPh)$_2$·TMEDA (mp 106 °C, 0.423 g, 0.95 mmol, 63% yield).

^{1}H NMR ($CDCl_3$): δ 7.33−7.31 (m, 4H), 6.97−6.88 (m, 6H), 2.50 (s, 4H), 2.35 (s, 12H). ^{13}C NMR ($CDCl_3$): δ 133.3 (*m*-C), 129.1 (*o*-C), 128.8 (*p*-C), 124.5 (*ipso*-C), 57.7 (−N−CH_2), 47.7 (N−CH_3). Anal. Calcd for $C_{18}H_{26}CdN_2S_2$: C, 48.37; H, 5.86; N, 6.27. Found: C, 48.51; H, 6.02; N, 6.13.

Preparation of Cd(SePh)$_2$·TMEDA. An amount of 0.340 g (0.75 mmol) of $Me_3SiSePh$ in 20 mL of toluene was added to a mixture of 4 mL of TMEDA and 0.137 g (0.75 mmol) of $CdCl_2$ in 30 mL of toluene. The reaction mixture was stirred at room temperature for 8 h and subsequently filtered to remove a small amount of a white solid.. The amount of solvent was reduced to half of its volume under reduced pressure, and the solution was stored at −24 °C. Colorless crystals of Cd(SePh)$_2$·TMEDA were obtained (mp 127 °C, 0.285 g, 70% yield).

^{1}H NMR ($CDCl_3$): δ 7.49−7.47 (m, 4H), 6.95−6.86 (m, 6H), 2.53 (s, 4H), 2.34 (s, 12H). ^{13}C NMR ($CDCl_3$): δ 136.1 (*m*-C), 128.8 (*o*-C, *p*-C), 124.3 (*ipso*-C), 57.0 (−N−CH_2), 47.3 (N−CH_3). Anal. Calcd for $C_{18}H_{26}CdN_2Se_2$: C, 39.98; H, 4.85; N, 5.18. Found: C, 39.14; H, 4.92; N, 5.41.

Preparation of Cd(TePh)$_2$. A sample of 0.818 g (2.0 mmol) of diphenyl ditelluride was dissolved in 30 mL of THF, and the solution was cooled to −78 °C. An amount of 4.2 mL of a 1 M solution of Li[Et_3BH] was added, and the reaction mixture was stirred for 2 h. An amount of 0.51 mL (4.0 mmol) of Me_3SiCl was added to the solution, and the reaction mixture was stirred for 2 h and allowed to warm to room temperature. The resulting lithium chloride was removed by filtration. A colorless solution was obtained. A solution of 0.366 mg (2.0 mmol) of $CdCl_2$ in THF was added at −78 °C. The reaction was allowed to warm to room temperature within 12 h, and the solvent was removed under reduced pressure. An orange solid of Cd(TePh)$_2$ was obtained (0.345 g, 32% yield).

Preparation of Cd(TePh)$_2$·TMEDA. A suspension of 1.80 g (3.45 mmol) of Cd(TePh)$_2$ in 30 mL of toluene was stirred at room temperature, 2 mL of TMEDA was added, and the mixture was stirred for an additional 24 h. An amount of 15 mL of pyridine/octane (1:2, v/v) was added to the light yellow solution, and the solution was filtered. The filtrate was evaporated to dryness, and the residue was dissolved in 20 mL of toluene. The solution was filtered again, the toluene was removed under vacuum, and a light yellowish solid was obtained (mp 101 °C, 60% yield).

^{1}H NMR ($CDCl_3$): δ 7.74−7.72 (m, 4H), 7.15−7.07 (m, 6H), 2.41 (s, 4H), 2.29 (s, 12H). ^{13}C NMR ($CDCl_3$): δ 137.7 (*m*-C), 129.4 (*o*-C), 128.0 (*p*-C), not detected (*ipso*-C), 57.1 (−N−CH_2), 47.4 (N−CH_3). Anal. Calcd for $C_{18}H_{26}CdN_2Te_2$: C, 33.88; H, 4.11; N, 4.38. Found: C, 33.47; H, 4.37; N, 4.59.

Synthesis of the Nanocomposites. A mixture of 20 mg of Cd(EPh)$_2$·TMEDA (E = S, Se, Te) and 50 mg of calcined SBA-15 silica was heated to 140 °C for 4 h. The temperature was raised to 350 °C at a rate of 1 K/min, and the sample was kept at this temperature for 16 h. The product was cooled to room temperature under a constant flow of argon. It was washed twice with 20 mL of hexane to remove potentially remaining organic residues and dried under vacuum. A yellowish product was obtained for CdS@SBA-15, whereas gray powders were obtained for CdSe@SBA-15 and CdTe@SBA-15.

Calorimetric Measurements. An amount of 30 mg of Cd(EPh)$_2$·TMEDA (E = S, Se, Te) was placed in a DSC pan consisting of a Pt/Rh mantle and a Al_2O_3 inlay and covered with a Pt/Rh lid. The calorimeter was evacuated twice and filled with argon before the measurements. The measurements were carried out under a constant gentle flow of argon at a heating rate of 10 K/min.

(27) Bawendi, M. G.; Kortan, A. R.; Steigerwald, M. L.; Brus, L. E. *J. Chem. Phys*. **1989**, *91*, 7282.
(28) Ricolleau, C.; Audinet, L.; Gandais, M.; Gacoin, T. *Eur. Phys. J. D* **1999**, *9*, 565.
(29) Ricolleau, C.; Audinet, L.; Gandais, M.; Gacoin, T.; Boilot, J.-P.; Chamarro, M. *J. Cryst. Growth* **1996**, *159*, 861.
(30) Lincot, D.; Mokili, B.; Froment, M.; Cortès, R.; Bernard, J.-P.; Witz, C.; Lafait, J. *J. Phys. Chem. B* **1997**, *101*, 2174.

Summary

Organochalcogenides of the composition $Cd(XPh)_2 \cdot TMEDA$ proved to be useful and versatile single-source precursors for the synthesis of nanoscale particles of the whole family of cadmium chalcogenides CdX (X = S, Se, Te). Nanocomposites of the type CdX@SBA-15 were synthesized by melt infiltration of the mesopores of SBA-15 silica with the organochalcogenolate precursors and subsequent thermolysis of the precursor in the template. Following this protocol, we obtained CdS in the wurtzite structure, CdTe in the sphalerite structure, and CdSe as a polytype involving both. The nanocomposites were characterized by X-ray powder diffraction and by TEM, showing highly crystalline particles in the mesopores of the template. After removal of the silica host with an aqueous base, the crystallinity and morphology of the cadmium chalcogenide particles remained unchanged. These findings regarding the structural chemistry of the three cadmium chalcogenides nicely reflect the thermodynamic stability of these dimorphic compound semiconductors with wurtzite as the stable phase for CdS, zinc blende as the stable phase for CdTe, and a mixed polymorph for CdSe, where the difference in the energy content of the two dimorphs is negligible. Because this tendency is observed for the particles in the mesopores of SBA-15 just as in aqueous solution, it can be concluded that the walls of this template provide an environment of sufficient polarity to allow the small incorporated particles investigated here to adopt their thermodynamically controlled minimum. This new role of the silica template, not only to define the particle size by an appropriate pore size but also to control the volume crystal structure of the produced particles, opens a generally new and different aspect of tailoring particle properties by template-assisted syntheses of nanoparticles.

Acknowledgment. Financial support by the DFG (SCHL 529/2-1 and FR 1372/10-1, SPP 1165 "Nanowires and Nanotubes"), the Fonds der Chemischen Industrie, and the Dr. Otto-Röhm Gedächtnisstiftung is gratefully acknowledged.

Supporting Information Available: Crystal structures of $Cd(SPh)_2 \cdot TMEDA$ and $Cd(SePh)_2 \cdot TMEDA$ and details of the crystal structure determinations. This material is available free of charge via the Internet at http://pubs.acs.org.

IC050517H